Percolation thresholds on elongated lattices

Marrink, Siewert; Knackstedt, Mark A.

Published in:
Journal of Physics A%3A Mathematical and General

DOI:
10.1088/0305-4470/32/44/101

J. Phys. A: Math. Gen. **32** (1999) L461–L466. Printed in the UK PII: S0305-4470(99)07628-3

LETTER TO THE EDITOR

Percolation thresholds on elongated lattices

S J Marrink† and Mark A Knackstedt†‡

† Department of Applied Mathematics, Research School of Physical Sciences and Engineering, Australian National University, Canberra ACT 0200, Australia

‡ Australian Petroleum Cooperative Research Centre, University of New South Wales, Sydney, NSW 2052, Australia

Received 7 September 1999

Abstract. We investigate the percolation thresholds of both random and invasion percolation in two and three dimensions on elongated lattices; lattices with a geometry of $L^{d-1} \times nL$ in d dimensions, where n denotes the aspect ratio of the lattice. Scaling laws for the threshold and spanning cluster density for random percolation are derived and simulation confirms the behaviour. A direct relationship between thresholds obtained for random percolation and invasion percolation is given and verified numerically.

Important contributions to understanding two-phase flow observations in porous media and rock have been made using percolation theory [1–3]. Random percolation (RP) is relevant to two-phase displacement if the flow is very slow and the invading fluid is completely wetting. Invasion percolation (IP) is relevant when the invading fluid is completely nonwetting. Both variants of percolation have been used to explain the structure and the amounts of fluids in a two-phase displacement at breakthrough. The fractal structure of the invading fluid paths have been analysed and the properties of IP are believed to be consistent with RP. In spite of this the spanning clusters are not precisely the same, and no relationship between the cluster density at spanning in RP and the breakthrough threshold in IP is known. Estimates of IP thresholds are neglected, particularly in three dimensions, due to the large computational effort required when compared with RP.

In most studies of percolation theory a simple square or cubic geometry is considered. In many applications one must consider systems with nonquadratic and noncubic geometries. For example, in the petroleum industry, laboratory measurements (e.g., residual saturations, capillary pressure) are performed on rock cores of high aspect ratio. These measurements are then used as input to reservoir simulation models. The crucial parameter measured is the value of the critical thresholds.

Using scaling arguments and small-scale numerical simulations, Monetti and Albano [4] presented scaling laws for the percolation probability in an elongated geometry that depend on the aspect ratio n of the lattice. In this paper we derive new scaling laws for percolation properties of elongated lattices (ELs) in both two and three dimensions, and present simulation data to confirm the theoretical results. We also derive relationships between thresholds observed in RP and IP for ELs and verify the relationships numerically.

Using finite-size scaling arguments, Monetti and Albano assumed the expectation value of the percolation threshold $\langle p_c^{(n)}(L)\rangle \propto L^{-1/\nu} n^{-1/\nu}$ where ν is the critical exponent for the correlation length. We define a lattice in d dimensions of size L^d as a simple lattice (SL).

0305-4470/99/440461+06$30.00

Consider an EL consisting of n L^d SLs linked together in series. The probability $P_n(p, L)$ that an EL of aspect ratio n percolates below p is given by the product of independent probabilities: $P_n(p, L) = \{P(p, L)\}^n \times \{C(p, L)\}^{n-1}$, where $P(p, L)$ is the probability of having a spanning cluster on a SL at p, and $C(p, L)$ is the connection probability that the spanning clusters of two SLs are connected at the $(d-1)$-dimensional interface. We have measured the magnitude of the connection probability via extensive simulations and found that $C(p, L) \simeq P(p, L)$ in both two and three dimensions [5]. We therefore approximate the probability by

$$P_n(p, L) = [P(p, L)]^{2n-1}. \tag{1}$$

Assuming the distribution of percolation thresholds on a SL can be accurately described by a distribution of the form $ce^{(-x^a)}$ [6,7] where $x = (p_c - \langle p_c(L)\rangle)/b$, a, b, and c being constants, we can write the probability of having a spanning cluster in a SL at $p_c < p$ as

$$P(p, L) = c\int_0^p e^{(-x^a)}\,dp_c = bc\int_{x_0}^x e^{-x^a}\,dx \tag{2}$$

with $x = (p - \langle p_c(L)\rangle)/b$ and $x_0 = -\langle p_c(L)\rangle/b$. For large x, $P(p, L)$ can be approximated by

$$P(p, L) = 1 - F(x)e^{(-(x)^a)} \tag{3}$$

where $F(x) = \frac{bc}{a}x^{(1-a)}$ denotes an algebraic correction to the leading decay. Substituting equation (3) into equation (1) we obtain the function $P_n(p, L)$ which approaches a Heaviside step function for large n. The position of the step $x[step]$ can be estimated from $P_n(p, L) = 0.5$, which after a Taylor expansion around $1/n = 0$ gives

$$x[step] = \left[\ln\left(n - \frac{1}{2}\right) + (1-a)\ln x[step] + \ln\frac{2bc}{a\ln 2}\right]^{\frac{1}{a}}. \tag{4}$$

Neglecting the constants and the $\ln x$ term ($\ln x, \ln\frac{2bc}{a\ln 2} \ll \ln n$, $n \gg \frac{1}{2}$) the expression simplifies to the remarkable result

$$x[step] = [\ln n]^{\frac{1}{a}}. \tag{5}$$

Assuming [6,7] that the distribution of percolation thresholds is approximately Gaussian with a standard deviation $\sigma(L)$ ($a = 2, b = \sqrt{2}\sigma(L), c = \frac{1}{b\sqrt{\pi}}$) the expectation value of the percolation threshold on an EL, ${p_c}^{(n)}(L)$, is given by the simple prediction

$$\langle {p_c}^{(n)}(L)\rangle = \langle p_c(L)\rangle + \sqrt{2}\sigma(L)\sqrt{\ln n}. \tag{6}$$

Numerical results for random site percolation with free boundary conditions are given in figure 1 illustrating the n-dependent scaling of the percolation thresholds in three dimensions for a range of $16 < L < 80$. Results in two dimensions show the same scaling behaviour. The number of realizations for each L was chosen to obtain $p_c^{(n)}(L)$ to within a standard error of 10^{-4}. All the data appear to follow equation (6) closely and strongly deviate from the prediction of Monetti and Albano for $n > 4$.

Considering the n SLs of the EL independently, the local density X of the percolating cluster in each SL depends on the value of the percolation threshold ${p_c}^{(n)}(L)$ of the EL and on the percolation threshold $p_c(L)$ of the SL. We can distinguish three regimes:

$$X \propto L^{-\beta/\nu} \qquad [{p_c}^{(n)}(L) = p_c(L)] \tag{7}$$

$$X \propto ({p_c}^{(n)}(L) - p_c(L))^{\beta} \qquad [{p_c}^{(n)}(L) > p_c(L)] \tag{8}$$

$$X \propto {p_c}^{(n)}(L) \qquad [{p_c}^{(n)}(L) \gg p_c(L)] \tag{9}$$

where $\beta = \frac{5}{26}$ in two dimensions and $\beta = 0.41$ in three dimensions. As shown in the previous section, ${p_c}^{(n)}(L)$ is expected to be larger than $p_c(L)$, so all simple lattices other than the

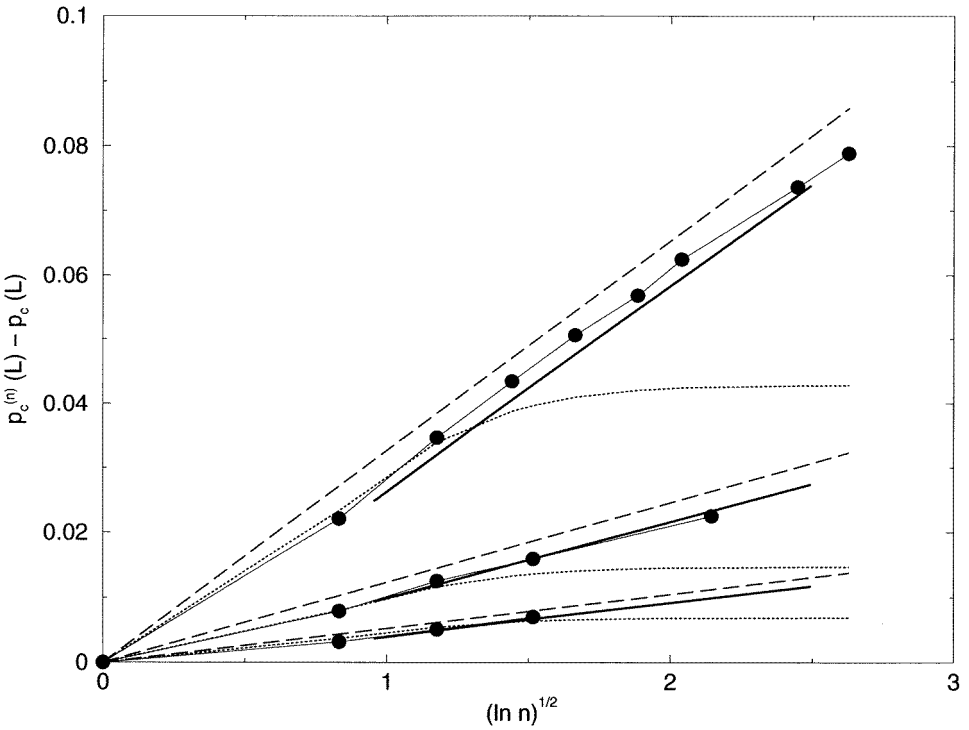

Figure 1. n-dependent scaling of the RP percolation threshold in three dimensions. From top to bottom the curves describe lattices with $L = 16$, 41 and 80. The thick solid lines are predictions of equation (1) (using a Gaussian fit of the percolation probability distribution of a SL), the dashed lines are the prediction of equation (6) and dotted curves give the prediction of Monetti and Albano.

'bottleneck' sublattice are above their percolation threshold. Therefore, the densities of the individual simple lattices are expected to scale according to either equation (8) or (9). Only the bottleneck sublattice scales according to equation (7).

For finite n and large L, ${p_c}^{(n)}(L)$ is still close to $p_c(L)$ and we expect most simple lattices to follow scaling law equation (8). Using equation (6) we obtain for the density $X_n(L)$ of the EL

$$X_n(L) \propto L^{-\beta/\nu}(\ln n)^{\beta/2}. \tag{10}$$

Figure 2 gives the n-dependent scaling behaviour of the density in three dimensions. The number of realizations was chosen to obtain standard errors in X_n of 10^{-3}. In this case the scaling relation given by equation (10) holds well over the range of n values studied. Results in two dimensions (not shown) are also consistent with equation (10).

At the breakthrough threshold for IP there is no analogue to the occupation probability p in RP as there are no finite clusters. The breakthrough threshold p_b is therefore analogous to the spanning cluster density at $X_n(L)$ in RP. We find that scaling similar to equation (10) for p_b is observed [5].

One can derive a relationship between the density of the spanning cluster in RP and the breakthrough threshold in IP for ELs. In RP, the location of the bottleneck within the EL has no influence on properties like the density. This, however, is no longer true in the case of IP. In IP if the bottleneck lattice is located at the *exit* face of the EL, then RP and IP will produce the same percolating cluster, as all sites with $p < p_b^{(1)}$ will be filled, where $p_b^{(1)}$ is the breakthrough

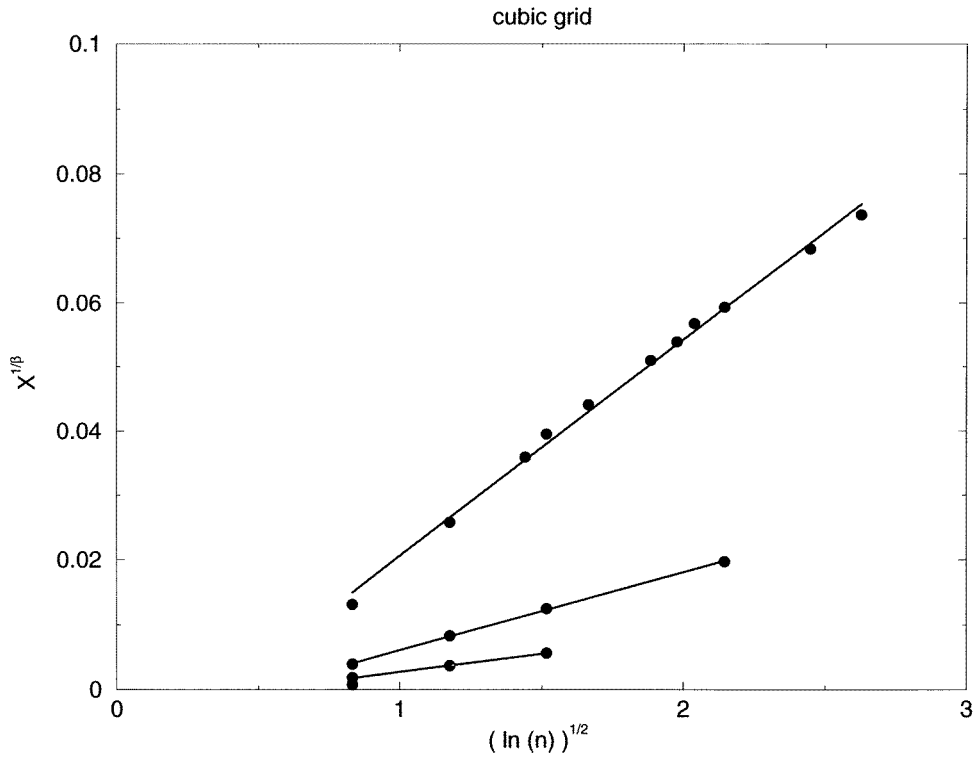

Figure 2. n-dependent scaling of the RP spanning cluster density in three dimensions. From top to bottom the curves describe lattices with $L = 16$, 41 and 80. Solid lines are predictions of equation (10).

threshold for the bottleneck lattice. However, if the bottleneck plane is located at some other position, then for the case of IP one finds sites with $p < p_b^{(1)}$ are occupied only up to the position of the bottleneck lattice. Beyond that, there is no need to fill sites up to $p = p_b^{(1)}$ and the density of the remainder of the lattice will be determined by a second bottleneck lattice, with occupation ${p_b}^{(2)} < p_b^{(1)}$. Repeating the argument, this part of the lattice again fills up sites with $p \leqslant {p_b}^{(2)}$ up to the position of this second bottleneck, after which a third bottleneck determines the occupation degree, etc.

In general, if the main bottleneck is located at a position i, where $1 < i \leqslant n$, then the densities up to position i are the same for IP and RP. The remainder of the lattice, having size $n-i$, fills up with a density corresponding to that of an EL with aspect ratio $n-i$. So the value of the density using IP given the position of the bottleneck at location i, denoted $X_n^{IP}[i]$, can be expressed as a weighted average of the expectation value of the density using RP, $\langle X_n^{RP}\rangle$ and the expectation value of the density using IP for a lattice with size $n-i$, $\langle X_{n-i}^{IP}\rangle$:

$$X_n^{IP}[i] = \frac{1}{n}(i\langle X_n^{RP}\rangle + (n-i)\langle X_{n-i}^{IP}\rangle). \tag{11}$$

The location i of the bottleneck within the EL could be anywhere, with equal probability. Considering an ensemble average over all possible locations of the bottleneck, we obtain, after some algebraic manipulation [5], the following expression:

$$\langle X_n^{IP}\rangle = \frac{1}{2n}\{(n+1)\langle X_n^{RP}\rangle + \langle X_{n-1}^{RP}\rangle + \langle X_{n-2}^{RP}\rangle + \cdots + \langle X_1^{RP}\rangle\} \tag{12}$$

where we assume $X_1^{IP} = X_1^{RP}$. Replacing the summation by an integral, we have

$$\langle X_n^{IP} \rangle = \frac{1}{2}\langle X_n^{RP} \rangle + \frac{1}{2n}\int_{i=1}^{n} \langle X_i^{RP} \rangle \, \mathrm{d}i \tag{13}$$

which provides for an easy conversion between densities obtained using RP versus IP.

Using the above equation it can be shown [5] that the expected difference between the density obtained with RP and IP vanishes in the limit of large n as

$$\langle X_n^{IP} \rangle - \langle X_n^{RP} \rangle \propto n^{-1}. \tag{14}$$

IP simulations begin by assigning an uncorrelated random number to each site on the lattice from an arbitrary distribution. Initially, the lattice is filled with the defending phase and the invading phase occupies one edge or face of the lattice. At each step in the simulation the site with the largest value on the interface between the invading and defending phases is displaced by the invader. The breakthrough threshold p_b is defined when the invading phase spans the lattice. As we are motivated by laboratory two-phase flow measurements on rock cores we consider free boundary conditions and results reported are measured over the full lattice. Again we consider thresholds along the direction of extension.

Figure 3 displays percolation results for the n-dependent scaling of the percolation threshold of ELs, both for RP and IP in three dimensions. Results on two-dimensional lattices show the same behaviour. Also shown is the theoretical prediction of the IP results according to equation (13), where the integral is solved numerically by interpolating the percolation results

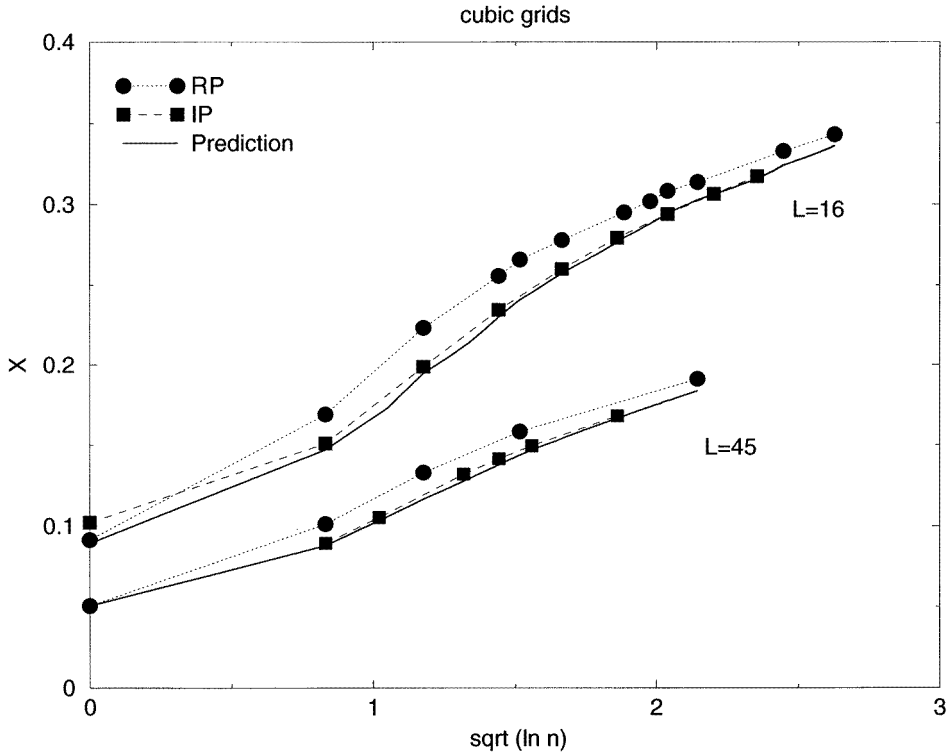

Figure 3. n-dependent scaling of the percolation threshold for ELs for RP and for IP in three dimensions. The theoretical prediction is obtained by numerically integrating equation (13) and using percolation results for RP.

for RP. From these data it is clear that the theoretically derived formula accurately predicts the difference between RP and IP densities. It also shows the convergence of RP and IP results in the limit of large n, as predicted by equation (14).

MAK is grateful to the Australian Research Council for financial support. We thank ANU Supercomputing Facility for allocations of computer time.

References

[1] Larson R, Scriven L E and Davis H T 1977 *Nature* **268** 409
[2] Stauffer D and Aharony A 1994 *Introduction to Percolation Theory* 2nd edn (London: Taylor and Francis)
[3] Sahimi M 1994 *Applications of Percolation Theory* 1st edn (London: Taylor and Francis)
[4] Monetti R A and Albano E V 1991 *Z. Phys.* B **82** 129
[5] Marrink S J and Knackstedt M 1999 to be submitted
[6] Ziff R M 1994 *Phys. Rev. Lett.* **72** 1942
[7] Haas U 1995 *Physica* A **215** 247